Environmental Science Nano

Detection and quantification of anthropogenic titanium, cerium, and lanthanum-bearing particles home dust

Journal:	*Environmental Science: Nano*
Manuscript ID	EN-ART-09-2022-000890.R1
Article Type:	Paper

Environmental Significance

Engineered particles are widely found in the indoor environment; however, there is currently no data on their concentrations in home dusts. Therefore, this study investigated the concentrations and size distributions of Ti, Ce, and La-bearing particles in home dusts collected from the surface of heating, ventilation, and air conditioning (HVAC) filters. The anthropogenic Ti, Ce, and La vary between 0 and 8,000, 0 and 6, 0 and 21 mg kg^{-1}, respectively. Whereas Ti occur predominantly as part of large fragments, La occur predominantly as nanosized particles. Anthropogenic Ti, Ce, and La concentrations in home dust are attributed to releases from paint, in particular during home renovation. The findings of this study imply the exposure of construction workers and residents to Ti, Ce, and La-bearing particles, in particular during home renovation, which may potentially pose human health risks.

Detection and quantification of anthropogenic titanium, cerium, and lanthanum-bearing particles home dust

Md Mahmudun Nabi, Jingjing Wang, and Mohammed Baalousha*

Center for Environmental Nanoscience and Risk, Department of Environmental Health Sciences, Arnold School of Public Health, University of South Carolina, Columbia, South Carolina, United States

* Corresponding author: mbaalous@mailbox.sc.edu

Abstract

Home dusts were collected from the surface of heating, ventilation, and air conditioning (HVAC) filters from eleven homes at different locations in Columbia, South Carolina, United States. Bulk metal concentrations in the dusts were measured using inductively coupled plasma-mass spectrometery (ICP-MS). Size-based elemental distributions in the < 450 nm particles were determined by asymmetrical flow-field flow fractionation (AF4) coupled to ICP-MS. The bulk Ti/Nb ratios are generally higher (up to 5,609) than the natural background ratios (*e.g.,* 320), indicating contamination of home dusts with TiO_2 engineered particles. Size-based Ti/Nb ratios in the < 450 nm fraction are similar to the natural background ratio, indicating a natural origin of Ti-bearing particles in this size fraction, and subsequently that anthropogenic Ti-bearing particles (TiO_2) are associated with particles > 450 nm either due to aggregation or to their release as large particles. The concentrations of TiO_2 engineered particles were estimated by mass balance calculations using total Ti concentrations and increases in Ti/Nb ratios above the natural background ratio. They vary between 0 and 13,300 mg TiO_2 kg^{-1}. The upper crustal-normalized rare earth element pattern indicates a positive La and Ce anomaly. The size of the cerium and lanthanum anomalies vary from 0.8 to 1.6 and 0.7 to 3.95, respectively, indicating contamination of several home dusts with Ce and La. The concentrations of bulk anthropogenic Ce and La were estimated based on mass balance calculations and anomaly size and varied between 0 and 5.7 ± 2.2 mg Ce kg^{-1} and 0 and 21.1 ± 7.4 mg La kg^{-1}, respectively. Size based Ce/La ratios in the < 450 nm fraction are lower than the natural background ratio, indicating contamination of this size fraction with nanosized La-bearing particles. Anthropogenic Ti and La concentrations in home dust are attributed to releases from paint during home renovation. This implies the exposure of construction workers to Ti and La-bearing particles during home renovation, which may potentially pose human health risks.

1. Introduction

Human exposure to indoor contaminants is an emerging area of health concern, especially because people spend up to 90% of their time indoors [1–3]. In developed countries, people spend approximately 65% of their daily time at home, with the young and elderly spending even more time at home [4,5]. Indoor dust accumulates environmental contaminants over extended periods, and thus has the potential to be used for retrospective exposure assessment. Many studies have investigated indoor dust to detect human exposure to a variety of chemical, physical, biological, and radiological contaminants [6]. Indoor dust is a complex mixture of particulate matter derived from a range of indoor and outdoor sources, which acts as both a sink and transport medium for contaminants such as metals and nanomaterials [7]. Indoor sources of particles include paint, renovation, cooking, indoor combustion, smoking, vaping, secondary formation processes, and dust resuspension [8–14]. Outdoor (atmospheric) particles in the urban environment originates predominantly from fossil fuel burning, automobile emissions, resuspension, or chemical and thermodynamic processes, but also from long range transport [15].

Several studies determined the concentrations of metals in home dust/particulate matter [16]. However, information on the occurrence and concentrations of metal-bearing nanomaterials in home dust remains scarce [14,17,18]. Several studies have investigated bulk metal concentrations in the fine and submicron fractions of indoor particulate matter (PM) [19,20]. Bari et al. identified dust resuspended from carpets as a source of Sb, electrical appliances as a source of Cu, and consumer products as a source of Ag in very fine particulate matter (PM_1 < 1 μm) in homes [19]. Suryawanshi et al. identified wall dust (*i.e.,* coatings and building materials) as a major source of indoor metal pollution and as a source of Ca, Cu, Fe, Pb, Mg and Ni in particulate matter < 0.6 μm ($PM_{0.6}$) [20]. Other studies investigated particulate matter composition at the single particle level using electron microscopy and energy dispersive X-ray spectroscopy [17,18]. Conner et al. identified cosmetics and personal care products as a possible source of several elements in indoor ($PM_{2.5}$ < 2.5 μm), including Al, Bi, Ti, Mg, Si and Fe [17]. Calderón et al. identified consumer spray products as a source of nanoscale (< 100 nm) and coarse aerosol particles (> 2.5 μm) containing Ag, Zn, Li, Sr, Ba, Pb, Mn, as well as other elements [18]. Other studies, using x-ray microanalysis, demonstrated that metals accumulate in house dust from common building materials and products such as Pb solder, As- and Cr-treated wood, and paint pigments containing Zn, Ti, Cr, Pb and Ba [14,21–24].

The detection of anthropogenic particles in environmental samples is complicated by the similarity of their physicochemical properties - such as size, shape, and elemental composition - to those of natural particles [25,26]. Thus, analytical approaches are being developed to differentiate natural from anthropogenic particles [25,27–29]. These approaches include bulk elemental ratio analysis (*e.g.,* Ce/La [25,30,31] and Ti/Nb [32–37]), size-based elemental ratio analysis [38,39], single particle elemental fingerprinting [40–43], and morphological analysis using electron microscopy [34,38,44]. For instance, the single particle elemental fingerprinting by single particle-inductively coupled plasma-mass spectrometry (SP-ICP-MS) is limited by the minimal detectable masses, which are element dependent [45]. Thus, nanomaterials with masses smaller than the minimal detectable masses cannot be characterized by SP-ICP-MS. Additionally, it is not possible to differentiate a true single element particle from a multi-element particle containing natural tracers with concentrations smaller than the minimal detectable mass using multi-element single particle analysis [46]. Morphological analysis of nanomaterials, typically performed using transmission electron microscopy (TEM), suffer poor statistical power due to limited number of particles that can be imaged and analyzed within a reasonable time and cost frame [47,48]. The bulk and size-based elemental ratio approach can be hampered by the co-contamination with the element of interest and the reference element (*e.g.,* co-contamination with Ce and La). In the case of co-contamination with rate earth elements, another approach that can be applied to differentiating natural from anthropogenic REEs is the normalization of REE concentrations to the upper crustal concentrations and the determination of rare earth element (REE) anomalies [49,50]. Normalization of REE concentrations in a given sample to the corresponding upper crustal REE concentrations removes the natural variations in absolute REE concentrations, resulting in a smooth REE pattern. Perturbances/spikes in the normalized REE concentration profile allows the identification of enrichment with a given REE.

The aims of this study are to: **(1)** determine anthropogenic Ti, Ce, and La concentrations in home dust, and **(2)** determine the particle size distribution of anthropogenic Ti, Ce, and La in-home dust. To this end, home dusts were collected from the surface of heating, ventilation, and air conditioning (HVAC) filters from eleven homes at different locations in Columbia, South Carolina, United States. Home dusts were analyzed for bulk metal concentrations following digestion by inductively coupled plasma-mass spectrometry (ICP-MS) and size-based elemental distributions by asymmetrical flow-field flow fractionation (AF4) coupled to ICP-MS, from which bulk and size-based elemental ratios were determined. Anthropogenic

elemental/particle concentrations were determined by mass balance calculations and shifts in elemental ratios above the natural background ratios and the size of REE anomalies.

2. Materials and Methods

2.1. Sampling and Analysis

Dust samples were collected from the surface of the HVAC filters from eleven different homes in Columbia, SC (**Figure S1**). Dust samples were gently scraped from the surface filters, placed in a 50 mL acid-washed test tube, which was sealed in a ziplock bag, labeled and returned to the laboratory. No information was available about the type of the filters used in these homes. Therefore, five different HVAC filters were purchased as a potentially representative group of HVAC filters used in homes including basic pleated (BP), advanced allergen (AA), microparticle reduction (MR), allergen reduction (AR), and dust reduction (DA) air filter. These filters were used as blanks to measure metal concentrations in clean/unused HVAC filters. Small pieces (*ca.* 1 cm x 1cm) of the HVAC filters were cut using a pair of clean ceramic scissors, placed inside the Teflon vessels (Savillex, Eden Prairie, MN, United States) in airtight condition, and then digested according to the same procedure used for the digestion of the dust samples.

2.2. Sample Digestion and Elemental Analysis

Dust samples were fully digested using a mixture of reagents, including H_2O_2, HNO_3, and HF, using modified method from our previous study [51]. Due to the high organic content, 25 or 50 mg dust samples were treated with 1 mL of 30% H_2O_2 (Fisher Chemical, Fair Lawn, NJ, United States) at 70 °C, then completely dried at 110 °C. The process was repeated twice to fully remove organic matter. Then, the residue was digested using distilled HF: HNO_3 (1:3) mixture (ACS grade acids distilled in the laboratory, Sigma Aldrich, St. Louis, MO, United States) at 110 °C for 48 h. Additional distilled HNO_3 was added to the samples to break down any insoluble fluoride salts. At the end of the digestion procedure, the samples were transferred to acid-prewashed centrifuge tubes using 1% trace metal grade HNO_3. Clean/unused HVAC filter pieces also were digested following the same procedure described above to determine the metal content in the HVAC filters themselves. USGS reference material—BHVO-2 Hawaiian basalts—was

digested using the same procedure to verify the method accuracy. All digested samples were stored at 4 °C before analysis.

Elemental concentrations were measured using Perkin Elmer NexION 350D ICP-MS (Perkin Elmer, Waltham, MA, USA) after routine standard tuning procedure. Instrument operating parameters are listed in **Table S1**. The monitored isotopes are listed in **Table S2**. Calibration curves for the monitored isotopes were established by measuring a series of ICP standards (BDH Chemicals, Radnor, PA, USA) with concentrations ranging from 0.01 to 1000 mg L^{-1}. Internal standard (5 µg L^{-1} Li, Sc, Y, In, Tb, and Bi in 1 % HNO_3, ICP Internal Element Group Calibration Standard, BDH Chemicals, Radnor, PA, USA) was measured as independent samples after each water sample to monitor any signal drift. No drift was observed for the internal standards throughout the analysis time. All data was collected using Syngistix 1.0. Elemental analysis of digested USGS reference materials BHVO-2 demonstrate the high recovery, accuracy, and precision for most elements (**Table S2**), confirming the reliability of the method.

2.3. Nanomaterial Extraction and Size Distribution

The < 450 nm size fraction was extracted from the home dusts following the procedure described in detail in our previous study [51]. Briefly, dusts were suspended in 10 mM tetrasodium pyrophosphate at pH=10 for 24 h by overhead 360-degree rotation. Then, the < 450 nm size fraction was separated by centrifugation (Eppendorf, 5810 R, Hamburg, Germany) at 775 g for 25 min (<450 nm assuming natural particle density, ρ = 2.5 g cm^{-3}) to prevent clogging of the ICP- MS introduction system.

The extracted suspensions were fractionated based on the particle diffusion coefficient—and thus equivalent spherical hydrodynamic diameter—using Wyatt Eclipse DualTec asymmetrical flow-field flow fractionation (AF4, Wyatt Technology Corporation, Santa Barbara, CA, USA). The AF4 channel characteristics and fractionation parameters are summarized in **Table S3**. The AF4 carrier phase consist of 10 mM $NaNO_3$, 0.0125% FL-70surfactant, and 0.01% NaN_3, a typical carrier phase used for the fractionation of natural and engineered nanomaterials [52,53]. The 10 mM $NaNO_3$ is used to partially screen the AF membrane surface charge, without inducing nanomaterial aggregation, and thus to minimize the impact of membrane- nanomaterial electrostatic interactions on nanomaterial separation. The FL-70 surfactant is used to prevent/minimize nanomaterial aggregation. NaN_3 is used to prevent any potential

biological growth in the AF4 channel. The elemental concentrations of the fractionated particles were then measured via an on-line ICP-MS. Prior to sample analysis, both AF4 and ICP-MS were tuned and calibrated separately. A Y-connector (PEEK, Analytical Sales & Services, Flanders, NJ, United States) was used to mix the AF4 effluent or the ICP-MS calibration standard (prepared in AF4 carrier phase)with the internal standard (5 μg L^{-1} Li, Sc, Y, In, Tb, and Bi in 2% HNO_3) at a 1:1 v:v ratio and to transport the mixture into the ICP-MS. In order to eliminate carryover, a 20-min 1% HNO_3 (Trace Metal Grade, Fisher Chemical, Fair Lawn, NJ, United States) rinse followed by a 10-min UPW rinse were applied between samples. AF4-ICP-MS data was collected using Chromera 4.1.0.6386 software.

2.4. Estimation of Anthropogenic Ti Concentration

The concentration of anthropogenic Ti was estimated based on mass balance calculations according to Eq. 1

$$Anthropogenic\ Ti = \left[Ti_{dust} - Nb_{dust}.\left(\frac{Ti}{Nb}\right)_{background}\right] \quad \text{(Eq. 1)}$$

Where, Ti_{dust} and Nb_{dust} are the concentrations of Ti and Nb in a given dust sample, $Ti/Nb_{background}$ is the natural background elemental concentration ratio of Ti/Nb. Here, we used the average crustal Ti/Nb of 320 as the natural background ratio [54].

2.5. Rare Earth Element Anomalies and Estimation of Anthropogenic Ce and La Concentrations

Shale normalized REE concentration (REE_n) patterns are a representation of the measured concentrations of REEs in a given sample divided by their respective concentrations in a reference shale plotted against atomic number. Here, we normalized the REE concentrations in the home dusts to the average upper crustal REE concentrations reported by Rudnick et al [54]. For uncontaminated samples, the crustal normalized REE patterns are smooth. On contrast, the crustal normalized REE patterns exhibit anomalous increases/decreases relative to the overall pattern for REEs with anthropogenic contributions.

Determining the size of the REE anomaly (REE_n/REE_n^*) in contaminated samples can be complicated by sample co-contamination with several neighboring REEs. The principal requirement for calculating REE anomalies is that the near neighbors used in the calculations must not show any anomalous behavior themselves. For example, for the calculation of La* we cannot use Ce_n as

contamination with Ce will affect the calculation of La* and vice versa. As a result, La and Ce anomalies were calculated using nearest available non-anomalous REEs (*e.g.,* Pr_n and Nd_n) according to Eqs. 2 and 3 [55].

$$La^* = \mathrm{Pr}_n * \left({Pr_n}/{Nd_n}\right)^2 \quad \text{(Eq. 2)}$$

$$Ce^* = \mathrm{Pr}_n * \left({Pr_n}/{Nd_n}\right) \quad \text{(Eq. 3)}$$

The anthropogenic REE concentration (REE_{Anth}) is then calculated using Eq 4 [56]

$$[REE_{Anth}] = \frac{\left(\frac{REE}{REE_n^*} - 1\right)}{\left(\frac{REE}{REE_n^*}\right)} * [REE_{measured}] \quad \text{(Eq. 4)}$$

Where [$REE_{Measured}$] is the measured of REE concentration in the dust samples.

3. Results and Discussion

3.1. Metals in House Dust

The concentrations of the 34 elements measured in the eleven home dusts are presented in **Figure S2**. Overall, Al, Fe, Ti, and Mn display the highest concentrations in all dusts and their concentration vary from few mg kg^{-1} to several thousands of mg kg^{-1} (**Figure S2a**). The concentrations of Zn, Zr, Cu, and Ba vary from few mg kg^{-1} to several hundreds of mg kg^{-1} (**Figure S2b**). The concentrations of Sr, Cr, Ni, Pb, V, Mo, Hf, and Co vary from sub mg kg^{-1} to several tens of mg kg^{-1} (**Figure S2c**). The concentrations of Nb, Th and Ta vary from sub mg kg^{-1} to few mg kg^{-1} (**Figure S2d**). The concentrations of REEs vary from sub mg kg^{-1} to few tens of mg kg^{-1} (**Figure S2e and f**). These elements could originate from natural sources such as soil particles or from anthropogenic sources such as road dust, or releases from building materials, appliances, and furniture [57–60].

Different home dusts are characterized by high concentrations of certain elements (**Figure S2**). For instance, dust from home 4 is characterized by higher Mn, Cr, Ni, V, Mo, and Co concentrations than all

other dust samples. Dust from home 8 is characterized by higher Ti, Sr, Ce, and La concentrations than all other dust samples. Dust from home 7 is characterized by higher Ti and Pb than all other dust samples. Dust from home 11 is characterized by higher concentrations of Al, Fe, Zn, Cu, Ba, Ni, V, Pb, Nb, Th, and all the REEs than all other dust samples. Below, we focus on few of these elements including Ti, Ce, and La, and we attempt to differentiate natural from anthropogenic sources of these elements and estimate their concentrations using mass balance calculations.

3.2. Anthropogenic Titanium Concentrations

The concentrations of Ti in home dusts vary between 161 ± 32 and 8,464 ± 660 mg kg^{-1} (**Figure 1a**). The Ti concentrations measured in the current study are higher than those reported (*e.g.,* 2,000 ± 995 mg kg^{-1}) in home dust in Christchurch, New Zealand [61] and Jersey City, New Jersey, USA households (*e.g.,* 1,060 ± 160 mg kg^{-1} to 1,640 ± 245 mg kg^{-1}) [62]. However, it is worth noting that the Ti concentration in some of the blank filters were also high and rang from 0.7 ± 0.6 to 1,952 ± 283 mg kg^{-1}. Nonetheless, the Ti concentrations in home dust 7 and 8 are respectively 1.5 and 5 fold higher than the highest Ti concentration in the five blank filters. The concentration of Ti in all other home dusts were lower than the maximum Ti concentration detected in the blank filters. These filters don't necessarily match the ones used in the homes from which the dust was collected but represent a range of common air filters in the market. The Ti/Nb ratio in the blank filters varied between 126 ± 77 to 231,536 ± 23715. The Ti/Nb ratio in all blank filters, except the basic pleated, was higher than the natural background Ti/Nb ratio (**Figure S3**), indicating the presence of anthropogenic TiO_2 particles in the blank filters. The high Ti concentrations in the blank filters are most likely due to the use of TiO_2 pigment as whitening agent in air filters. Despite the high TiO_2 concentrations in some of the blank HVAC filters, their contribution to the dust samples should be limited as we gently scrapped the dust samples from the HVAC filter surface and made all possible attempts to minimize the contribution of the HVAC filter material to the dust samples. Thus, we estimate that the majority of the anthropogenic Ti in the dust samples, in particular those collected from home 7 and 8, are attributed to the dust itself rather than the filter material.

The Ti/Nb ratio in all the home dust samples vary between 227 ± 6 and 5,609 ± 1048. The Ti/Nb in all home dusts, except home dust 4, is higher than the natural background ratio, indicating anthropogenic Ti

contamination (**Figure 1b**). The anthropogenic Ti concentration was estimated to vary between 0 and 7,974 ± 677 mg kg^{-1} (**Figure 1c**). Assuming that anthropogenic Ti is due to pure TiO_2 engineered particles, the anthropogenic Ti concentration corresponds to 0 to 13,304 ± 1,129 mg TiO_2 kg^{-1} with the highest concentration in home 8, which was renovated (re-painted) prior to sample collection. Therefore, the high TiO_2 concentration in home number 8 can be attributed to release of TiO_2 from paint sanding, given that TiO_2 is the most widely used as a pigment in paints [63]. This is consistent with previous studies that demonstrated the occurrence of metal-bearing particles in home dust [14]. For instance, using micro-X-ray fluorescence and micro-X-ray diffraction approaches, Walker et al identified Ti, Pb, Zn, Ba, Cr, Cu -bearing particles in home dust, and attributed these particles to pigments released from paint during renovation activities because of the presence of lithopone (a mixture of barite and wurtzite), zinc oxide (zincite), hydrocerussite, rutile, and anatase [14]. Furthermore, recent trends to incorporate nano–size additives (*e.g.,* SiO_2, Fe_2O_3, SiO_2 and TiO_2) within concrete (to improve workability and strength) introduce additional source of engineered particles, which could be released during demolition and recycling [54]. Demolition and construction activities associated with building renovation are known to produce substantial amounts of particulate matter (PM), including coarse (PM_{10} ≤ 10 μm), fine ($PM_{2.5}$ ≤ 2.5 μm), very fine (PM_1 ≤ 1 μm), and ultrafine particles (UFP ≤ 100 nm) [64,65]. The UFPs were found to account for > 90% of the total particle number concentrations and <10% of the total mass concentration released during renovation activities such as wall-chasing, drilling, cementing, and general demolition activities [66]. The absence of anthropogenic TiO_2 in home dust 4 is ascribed to the fact that this home is located in a remote area and did not undergo any paint or renovation works in the recent years.

3.3. Anthropogenic Cerium and Lanthanum Concentrations

Ce and La concentrations vary from 0.8 ± 0.1 to 16.9 ± 3.7 and 0.4 ± 0.05 to 28.6 ± 6.5 mg kg^{-1}, respectively (**Figure 2**). These concentrations are much higher than those detected in the blank filters (**Table S4**). The Ce concentrations in the blank filters vary between 0 and 0.1 ± 0.2 mg kg^{-1}. Lanthanum concentrations in the blank filters are below the ICP-MS limit of detection (0.0096 μg L^{-1}). All dusts, other than those collected from homes 6 and 8, display higher Ce than La concentrations. This gives an initial indication of La contamination in dust 6 and 8, given that Ce is two fold more abundant than La in the upper

earth crust [54]. Below, we describe how we identified and quantified anthropogenic Ce and La contaminations in the dust samples.

First, we explored the crustal normalized REE pattens in the dust samples. Crustal normalized REE concentrations of a non-contaminated environmental samples are well known to display a smooth pattern [67,68]. Perturbances/spikes in the normalized REE profile indicate probable REE contamination since the normalization removes the natural variations in absolute concentrations of REEs. From this point of view, spikes in the normalized REE concentration profile can be used as markers of anthropogenic contamination in dust samples. Overall, home dusts are characterized by elevated REE concentrations relative to the upper crustal average concentrations and to the clean filters (**Figures 3 and S4**). The overall patterns of the upper crustal normalized REEs in dusts from homes 1, 2, 3, 4, 5, 9, 10, and 11 are uniform and display a similar pattern to upper average crust (**Figure 3a**), indicating that the REEs in these dusts originate from natural sources. In contrast, the upper crustal normalized REE profile in dust samples from homes 6, 7, and 8 show enrichment in Ce, and La (**Figure 3b**, with the dust from home 8 showing the highest enrichment in Ce and La, indicating that dust from these homes originate from a mix of natural and anthropogenic sources. In particular, the pattern of upper crustal normalized REEs in dust 8 is strongly perturbed.

Elemental ratios of Ce to La in the bulk dust samples varied from 0.6 to 2.2 indicating possible Ce and La contamination in home dusts (**Figure 4a**). More specifically, Ce/La in dusts collected from home 1 and 4 have slightly higher elemental ratios than the upper crustal value (i.e., 2.0), suggesting that dust from these homes might potentially be contaminated with Ce. Additionally, Ce/La in dusts from homes 2, and 6 to 10 have lower ratios compared to the upper crustal value—with lowest ratios in dusts from homes 6 and 8, suggesting that dusts from these homes are potentially contaminated with La. Given that the dust samples might be contaminated with both Ce and La and that Nd (the next most abundance REE after Ce and La) does not seem to be enriched in any of the dust samples (**Figure 3**), we calculated the elemental ratios of Ce/Nd and La/Nd (**Figure 4b and c**). The elemental ratios of Ce/Nd (**Figure 4b**) indicate that dust from homes 1, 3, 7, 8, 9, 10, and 11 have higher values than the average crustal value (*i.e.,* 2.33)—with the highest Ce/Nd of 6.5 measured in the home dust 8— indicating that dusts from these homes are potentially contaminated with Ce. The La/Nd (**Figure 4c**) indicate that dust from homes 6, 7, 8, 9 and 10

have higher values than the average crustal value (i.e., 1.15)—with the highest La/Nd of 11.3 measured in the home dust 8— indicating that dusts from these homes are potentially contaminated with La. The dust from home 8 exhibited the lowest Ce/La and the highest Ce/Nd and La/Nd, indicating that this dust is most likely contaminated with both Ce and La.

An alternative approach to elemental ratio analysis is based on calculating the size of REE anomalies in order to identify and quantify anthropogenic REE concentrations [56]. The size of Ce and La anomalies (Ce/Ce* and La/La*, **Figure 5a and b**) vary from 0.8 to 1.64 and 0.8 to 3.95, indicating that several home dusts are contaminated with Ce and La. The sizes of Ce anomalies are < 1.5 for all dusts except home 8 and 10, for which Ce anomalies are 1.5 and 1.64, indicating potential contamination with Ce in these two homes. The sizes of La anomalies are < 1.5 in all dust samples except dust from home 6, 8 and 10, for which La anomalies are 1.66, 3.95, and 1.74, respectively, indicating that dust homes 6, 8 and 10 are contaminated with La. The estimated anthropogenic Ce and La concentrations vary between 0 and 5.7 ± 2.2 mg Ce kg^{-1} and 0 and 21.1 ± 7.4 mg La kg^{-1}, respectively (**Figure 5c and d**).

The high Ce and La concentrations in dust 8 are likely due to indoor emissions during the house renovation such as paint pigments and/or driers. La_2O_3 is used as a pigment in paint. Additionally, driers used in solvent-based and water-based paints containing unsaturated polymers are principally metal salts —lead, calcium, cobalt, manganese, cerium, and lanthanum— of naphthenic acid and neodecanoic acid [69,70]. Other uses of Ce and La within the indoor environment that could result in their releases, include the use of: cerium as the major component of mischmetal alloy (just under 50%) which is used in 'flints' for lighters; Ce_2O_3 as a catalyst in the inside walls of self-cleaning ovens to prevent the build-up of cooking residues; cerium in flat-screen TVs and low-energy light bulbs in the indoor environment [71,72]; La in equipment such as color televisions, fluorescent lamps, energy-saving lamps and glasses [72,73].

3.4. Elemental Size-based Distribution

Particles < 0.45 μm were extracted from dust with the lowest (home 4), intermediate (home 7), and highest (home 8) Ti/Nb and were analyzed by AF4-ICP-MS to determine their size-based elemental concentrations and ratio distributions (raw AF4-ICP-MS data are presented in **Figure S5**). The Ti/Nb ratios are approximately 300 in < 0.45 μm fractions for all dust samples (**Figure 6**), similar to those reported in

non-contaminated soil particles [31,51], indicating the absence of anthropogenic TiO_2 particles in the extracted suspensions. Thus, the high Ti/Nb in the bulk dust samples can be attributed to the contamination of the dust samples with large or heteroaggregated Ti-bearing particles. The high variability in Ti/Nb elemental ratios likely reflects low Nb concentrations (close to the limit of quantification) as it occurs at low concentrations in natural Ti-bearing minerals.

The elemental size distribution of Ce and La in the < 0.45 µm suspensions extracted from dusts from homes 4, 7 and 8 (no, low, and high La contamination) are presented in **Figure 7** and shows that Ce and La co-eluted in the size range of 1 to 100 nm. The Ce/La ratios in dusts 4 and 7 vary between 1 and 2, whereas those in dust 8 vary between 0.05 and 0.2. These results follow the same trend as the elemental ratios calculated on the bulk dust samples (**Figure 4a**). Furthermore, the elemental ratios of Ce/Nd and La/Nd are presented in **Figure 8**. The extracted suspensions exhibit Ce/Nd close to the average crustal values (**Figure 8a, c, and e**), whereas the elemental ratio of La/Nd exhibit higher values than the average crustal values in all dusts with slightly higher ratios in dusts from homes 4 and 7 (**Figure 8b and d**) and much higher ratios in dust from home 8 (**Figure 8c**), in good agreement with the bulk elemental ratio trends (**Figure 4c)**. These results indicate that there is no or small Ce contamination in all home dust samples, no or small La contamination in dust 4 and 7, and high La contamination in dust 8.

Whereas anthropogenic Ti occur as large particles > 450 nm, anthropogenic La-containing particles occur in the nano-sized particles (*e.g.,* < 60 nm, **Figure 7 and 8**). These differences might be attributed to the different sources of Ti and La or to the differences in the release of Ti and La from the same source. The likely source of anthropogenic Ti and La in dust 8 was the paint used during renovation. TiO_2 (100-300 nm) is the most widely used pigment in paints. Additionally, the use of 0.5-5% (w/w) nanomaterials (10-100 nm, including La_2O_3) remarkably improves the properties of paint in term of scratch resistance, hardness, gloss, weather stability, and cross linking and hardening properties [70]. Nanomaterials and pigments are present as single particles in paint only at the time of manufacturing. They increase in effective size by agglomeration and by absorption of polymers and surface-active agents onto their surface. During drying process, the particles continue to agglomerate and are incorporated irreversibly into the polymer matric [70]. It is worth noting that gray/white chunks were visually observed in the settled particles during the separation

of the < 450 nm size fraction, and qualitatively smaller quantities of these gray/white chunks were observed in dust 7 sediment. Thus, most likely TiO_2 particles were released as a component of paint fragments. In contrast, La_2O_3 were likely released as smaller aggregates/primary particles. The release of small La-bearing particles could also be attributed to the fact that surface functionalized La_2O_3 nanomaterials, using chemically bound polymers, allow for the La_2O_3 nanomaterials to be preferentially adsorbed at the surface interface in solvent-based and water-based paints [74].

4. Conclusions and Environmental Implications

This study investigated the occurrence of anthropogenic Ti, Ce, and La in eleven home dusts collected from the surface HVAC filters in Columbia, South Carolina, United States. To the best of our knowledge this study provides the first dataset on anthropogenic Ti, Ce, and La-bearing particle concentrations in home dusts. The concentration of anthropogenic titanium, cerium, and lanthanum varied between 0 to 8,000 mg Ti kg^{-1}, 0 to 6 mg Ce kg^{-1}, and 0 to 21 mg La kg^{-1}, respectively. Whereas anthropogenic Ti-bearing particles occurred as large particles > 450 nm, anthropogenic La-containing particles occurred in the nano-sized range. These differences in anthropogenic particle size could be attributed to the size of the used particles or to the nature of the released particles. The occurrence of these anthropogenic particles (likely as TiO_2, CeO_2 and La_2O_3) in home dust implies that these particles were suspended in the indoor air and thus are available for inhalation, and for transport to eating and food preparation areas. The high anthropogenic Ti and La concentrations (likely as TiO_2 and La_2O_3) in the renovated home dust imply the exposure of construction workers to high levels of these particles. Such high level of exposure is a potential hazard to human health. For instance, TiO_2 particles are likely to cause diseases to human, including tumors, cancer, and affect the brain, heart, intestinal mucosa, and other internal organs [75]. TiO_2 particles are classified as suspect carcinogen to human by inhalation [70]. Additionally, the use of TiO_2 as food additive has been recently banned by the European Union due to potential human health implications [26]. Reports on indoor air concentrations of Ce and La and their related health effects are scarce [76]. Nonetheless, occupational exposure to CeO_2 and La_2O_3 nanomaterials has been shown to results in the accumulation of cerium in the lungs and to cause lung diseases such as pneumoconiosis, endomyocardial fibrosis, and myocardial infarction [77–85]. Overall, the presence of these particles in home

dusts may pose indoor environment air quality and human health risks due to elongated and continuous exposure.

The findings of this study also have significant implications for the detection and quantification of engineered nanomaterials (*e.g.,* CeO_2 and La_2O_3) in environmental samples. For instance, the increases in the elemental ratios of Ce/La above the natural background ratios have been suggested as a proxy for the detection and quantification of CeO_2 NMs in environmental samples. However, the co-contamination of samples with both Ce and La may lead to erroneous results. In such a scenario, the use of alternative ratios such as Ce/Nd, La/Nd and Ce and La anomaly analysis provides an alternative tool to the elemental ratio of Ce to La.

5. Acknowledgment

This work was supported by US National Science Foundation CAREER (1553909) grant to Dr. Mohammed Baalousha.

6. Competing interest statement

The authors declare no competing interest

7. Author Contributions

Dr. Mohammed Baalousha conceived the overall idea of the research and coordinated sample collection. Mr. MD Mahmudun Nabi and Dr. Jingjing Wang performed all experimental work and data analysis. Mr. MD Mahmudun Nabi wrote the first draft. All authors contributed to the manuscript writing and editing.

1. Kurt-Karakus, P. B. Determination of heavy metals in indoor dust from Istanbul, Turkey: Estimation of the health risk. *Environ. Int.* **50**, 47–55 (2012).

2. Rasmussen, P. E. *et al.* Canadian House Dust Study: Population-based concentrations, loads and loading rates of arsenic, cadmium, chromium, copper, nickel, lead, and zinc inside urban homes. *Sci. Total Environ.* **443**, 520–529 (2013).

3. Yoshinaga, J. *et al.* Lead and other elements in house dust of Japanese residences – Source of lead and health risks due to metal exposure. *Environ. Pollut.* **189**, 223–228 (2014).

4. LEECH, J. A., NELSON, W. C., BURNETT, R. T., AARON, S. & RAIZENNE, M. E. It's about time: A comparison of Canadian and American time–activity patterns. *J. Expo. Sci. Environ. Epidemiol. 2002 126* **12**, 427–432 (2002).

5. Brasche, S. & Bischof, W. Daily time spent indoors in German homes – Baseline data for the assessment of indoor exposure of German occupants. *Int. J. Hyg. Environ. Health* **208**, 247–253 (2005).

6. Doyi, I. N. Y., Isley, C. F., Soltani, N. S. & Taylor, M. P. Human exposure and risk associated with trace element concentrations in indoor dust from Australian homes. *Environ. Int.* **133**, 105125 (2019).

7. Whitehead, T., Metayer, C., Buffler, P. & Rappaport, S. M. Estimating exposures to indoor contaminants using residential dust. *J. Expo. Sci. Environ. Epidemiol. 2011 216* **21**, 549–564 (2011).

8. Waring, M. S. Secondary organic aerosol in residences: predicting its fraction of fine particle mass and determinants of formation strength. *Indoor Air* **24**, 376–389 (2014).

9. Waring, M. S. & Siegel, J. A. An evaluation of the indoor air quality in bars before and after a smoking ban in Austin, Texas. *J. Expo. Sci. Environ. Epidemiol. 2007 173* **17**, 260–268 (2006).

10. Schripp, T., Markewitz, D., Uhde, E. & Salthammer, T. Does e-cigarette consumption cause passive vaping? *Indoor Air* **23**, 25–31 (2013).

11. Wallace, L. Indoor Sources of Ultrafine and Accumulation Mode Particles: Size Distributions, Size-

Resolved Concentrations, and Source Strengths. *Aerosol Sci. Technol.* **40**, 348–360 (2006).

12. Wallace, L. Indoor Particles: A Review. *J. Air Waste Manage. Assoc.* **46**, 98–126 (1996).

13. AA, A. H., IH, Y. & IM, K. Indoor air quality during renovation actions: a case study. *J. Environ. Monit.* **6**, 740–744 (2004).

14. Walker, S. R., Jamieson, H. E. & Rasmussen, P. E. Application of Synchrotron Microprobe Methods to Solid-Phase Speciation of Metals and Metalloids in House Dust. *Environ. Sci. Technol.* **45**, 8233–8240 (2011).

15. Belis, C. A., Karagulian, F., Larsen, B. R. & Hopke, P. K. Critical review and meta-analysis of ambient particulate matter source apportionment using receptor models in Europe. *Atmos. Environ.* **69**, 94–108 (2013).

16. Rasmussen, P. E., Levesque, C., Chénier, M. & Gardner, H. D. Contribution of metals in resuspended dust to indoor and personal inhalation exposures: Relationships between PM10 and settled dust. *Build. Environ.* **143**, 513–522 (2018).

17. Conner, T. L., Norris, G. A., Landis, M. S. & Williams, R. W. Individual particle analysis of indoor, outdoor, and community samples from the 1998 Baltimore particulate matter study. *Atmos. Environ.* **35**, 3935–3946 (2001).

18. Calderón, L. *et al.* Release of airborne particles and Ag and Zn compounds from nanotechnology-enabled consumer sprays: Implications for inhalation exposure. *Atmos. Environ.* **155**, 85–96 (2017).

19. Bari, M. A. *et al.* Indoor and Outdoor Levels and Sources of Submicron Particles (PM1) at Homes in Edmonton, Canada. *Environ. Sci. Technol.* **49**, 6419–6429 (2015).

20. Suryawanshi, S., Chauhan, A. S., Verma, R. & Gupta, T. Identification and quantification of indoor air pollutant sources within a residential academic campus. *Sci. Total Environ.* **569–570**, 46–52 (2016).

21. Rasmussen, P. E. *et al.* Impact of humidity on speciation and bioaccessibility of Pb, Zn, Co and Se in house dust. *J. Anal. At. Spectrom.* **29**, 1206–1217 (2014).

22. MacLean, L. C. W., Beauchemin, S. & Rasmussen, P. E. Lead Speciation in House Dust from Canadian Urban Homes Using EXAFS, Micro-XRF, and Micro-XRD. *Environ. Sci. Technol.* **45**, 5491–5497 (2011).

23. Beauchemin, S., Rasmussen, P. E., MacKinnon, T., Chénier, M. & Boros, K. Zinc in House Dust: Speciation, Bioaccessibility, and Impact of Humidity. *Environ. Sci. Technol.* **48**, 9022–9029 (2014).

24. Beauchemin, S., MacLean, L. C. W. & Rasmussen, P. E. Lead speciation in indoor dust: a case study to assess old paint contribution in a Canadian urban house. *Environ. Geochemistry Heal. 2011 334* **33**, 343–352 (2011).

25. F, von der K. *et al.* Analysis of engineered nanomaterials in complex matrices (environment and biota): general considerations and conceptual case studies. *Environ. Toxicol. Chem.* **31**, 32–49 (2012).

26. European Union Regulation Commission. *Amending Annexes II and III to Regulation (EC) No 1333/2008 of the European Parliament and of the Council as regards the food additive titanium dioxide (E 171)*. (2022).

27. Montaño, M. D. *et al.* Current status and future direction for examining engineered nanoparticles in natural systems. *Environ. Chem.* **11**, 351–366 (2014).

28. Slomberg, D. L. *et al.* Anthropogenic Release and Distribution of Titanium Dioxide Particles in a River Downstream of a Nanomaterial Manufacturer Industrial Site. *Front. Environ. Sci.* **0**, 76 (2020).

29. Mehrabi, K., Kaegi, R., Günther, D. & Gundlach-Graham, A. Emerging investigator series: automated single-nanoparticle quantification and classification: a holistic study of particles into and out of wastewater treatment plants in Switzerland. *Environ. Sci. Nano* **8**, 1211–1225 (2021).

30. Morera-Gómez, Y., Santamaría, J. M., Elustondo, D., Lasheras, E. & Alonso-Hernández, C. M. Determination and source apportionment of major and trace elements in atmospheric bulk deposition in a Caribbean rural area. *Atmos. Environ.* **202**, 93–104 (2019).

31. Yi, Z., Loosli, F., Wang, J., Berti, D. & Baalousha, M. How to distinguish natural versus engineered

nanomaterials: insights from the analysis of TiO2 and CeO2 in soils. *Environ. Chem. Lett.* **18**, 215–227 (2020).

32. Loosli, F. *et al.* Sewage spills are a major source of titanium dioxide engineered (nano)-particle release into the environment. *Environ. Sci. Nano* **6**, 763–777 (2019).

33. Nabi, M. M., Wang, J. & Baalousha, M. Episodic surges in titanium dioxide engineered particle concentrations in surface waters following rainfall events. *Chemosphere* **263**, 128261 (2021).

34. Wang, J. *et al.* Detection and quantification of engineered particles in urban runoff. *Chemosphere* **248**, 126070 (2020).

35. Baalousha, M., Wang, J., Erfani, M. & Goharian, E. Elemental fingerprints in natural nanomaterials determined using SP-ICP-TOF-MS and clustering analysis. *Sci. Total Environ.* **792**, 148426 (2021).

36. Nabi, M. M., Wang, J., Journey, C. A., Bradley, P. M. & Baalousha, M. Temporal variability in TiO2 engineered particle concentrations in rural Edisto River. *Chemosphere* **297**, 134091 (2022).

37. Feiyun Tou *et al.* Multi-method approach for analysis of road dust particles: elemental ratios, SP-ICP-TOF-MS, and TEM. *Environ. Sci. Nano* **12**, 2022 (2022).

38. Baalousha, M. *et al.* Stormwater green infrastructures retain high concentrations of TiO2 engineered (nano)-particles. *J. Hazard. Mater.* **392**, 122335 (2020).

39. Meili-Borovinskaya, O. *et al.* Analysis of complex particle mixtures by asymmetrical flow field-flow fractionation coupled to inductively coupled plasma time-of-flight mass spectrometry. *J. Chromatogr. A* **1641**, 461981 (2021).

40. Baalousha, M., Wang, J., Erfani, M. & Goharian, E. Elemental fingerprints in natural nanomaterials determined using SP-ICP-TOF-MS and clustering analysis. *Sci. Total Environ.* **792**, 148426 (2021).

41. Gondikas, A. *et al.* Where is the nano? Analytical approaches for the detection and quantification of TiO 2 engineered nanoparticles in surface waters. *Environ. Sci. Nano* **5**, 313–326 (2018).

42. Praetorius, A. *et al.* Single-particle multi-element fingerprinting (spMEF) using inductively-coupled

plasma time-of-flight mass spectrometry (ICP-TOFMS) to identify engineered nanoparticles against the elevated natural background in soils. *Environ. Sci. Nano* **4**, 307–314 (2017).

43. Gundlach-Graham, A. Multiplexed and multi-metal single-particle characterization with ICP-TOFMS. *Compr. Anal. Chem.* **93**, 69–101 (2021).

44. Kaegi, R. *et al.* Release of TiO 2 – (Nano) particles from construction and demolition landfills. *NanoImpact* **8**, 73–79 (2017).

45. Lee, S. *et al.* Nanoparticle size detection limits by single particle ICP-MS for 40 elements. *Environ. Sci. Technol.* **48**, 10291–10300 (2014).

46. Baalousha, M., Wang, J., Erfani, M. & Goharian, E. Elemental fingerprints in natural nanomaterials determined using SP-ICP-TOF-MS and clustering analysis. *Sci. Total Environ.* **792**, 148426 (2021).

47. Baalousha, M. *et al.* Characterization of cerium oxide nanoparticles—Part 1: Size measurements. *Environ. Toxicol. Chem.* **31**, 983–993 (2012).

48. Baalousha, M. *et al.* Characterization of cerium oxide nanoparticles—Part 2: Nonsize measurements. *Environ. Toxicol. Chem.* **31**, 994–1003 (2012).

49. Oppenheimer, J. A., Badruzzaman, M. & Jacangelo, J. G. Differentiating sources of anthropogenic loading to impaired water bodies utilizing ratios of sucralose and other microconstituents. *Water Res.* **46**, 5904–5916 (2012).

50. Knappe, A., Möller, P., Dulski, P. & Pekdeger, A. Positive gadolinium anomaly in surface water and ground water of the urban area Berlin, Germany. *Geochemistry* **65**, 167–189 (2005).

51. Loosli, F., Yi, Z., Wang, J. & Baalousha, M. Improved extraction efficiency of natural nanomaterials in soils to facilitate their characterization using a multimethod approach. *Sci. Total Environ.* **677**, 34–46 (2019).

52. Bednar, A. J. *et al.* Comparison of on-line detectors for field flow fractionation analysis of nanomaterials. *Talanta* **104**, 140–148 (2013).

53. Saenmuangchin, R. & Siripinyanond, A. Flow field-flow fractionation for hydrodynamic diameter estimation of gold nanoparticles with various types of surface coatings. *Anal. Bioanal. Chem.* **410**, 6845–6859 (2018).

54. Rudnick, R. L. & Fountain, D. M. Nature and composition of the continental crust: A lower crustal perspective. *Rev. Geophys.* **33**, 267 (1995).

55. Lawrence, M. G., Greig, A., Collerson, K. D. & Kamber, B. S. Rare Earth Element and Yttrium Variability in South East Queensland Waterways. doi:10.1007/s10498-005-4471-8

56. Lawrence, M. G., Ort, C. & Keller, J. Detection of anthropogenic gadolinium in treated wastewater in South East Queensland, Australia. *Water Res.* **43**, 3534–3540 (2009).

57. Hunt, A., Johnson, D. L. & Griffith, D. A. Mass transfer of soil indoors by track-in on footwear. *Sci. Total Environ.* **370**, 360–371 (2006).

58. Rasmussen, P. E., Subramanian, K. S. & Jessiman, B. J. A multi-element profile of house dust in relation to exterior dust and soils in the city of Ottawa, Canada. *Sci. Total Environ.* **267**, 125–140 (2001).

59. W, B. & B, H. Pollutants in house dust as indicators of indoor contamination. *Rev. Environ. Contam. Toxicol.* **175**, 1–46 (2002).

60. Lanzerstorfer, C. Variations in the composition of house dust by particle size. *http://dx.doi.org/10.1080/10934529.2017.1303316* **52**, 770–777 (2017).

61. Fergusson, J. E., Forbes, E. A., Schroeder, R. J. & Ryan, D. E. The elemental composition and sources of house dust and street dust. *Sci. Total Environ.* **50**, 217–221 (1986).

62. Wang, E. Y., Willis, R. D., Buckley, T. J., Rhoads, G. G. & Lioy, P. J. The Relationship Between the Dust Lead Concentration and the Particle Sizes of Household Dusts Collected in Jersey City Residences. *http://dx.doi.org/10.1080/1047322X.1996.10390605* **11**, 199–206 (2011).

63. Braun, J. H., Baidins, A. & Marganski, R. E. TiO2 pigment technology: a review. *Prog. Org. Coatings* **20**, 105–138 (1992).

64. Kumar, P., Mulheron, M., Fisher, B. & Harrison, R. M. New Directions: Airborne ultrafine particle dust from building activities – A source in need of quantification. *Atmos. Environ.* **56**, 262–264 (2012).

65. Kumar, P., Pirjola, L., Ketzel, M. & Harrison, R. M. Nanoparticle emissions from 11 non-vehicle exhaust sources – A review. *Atmos. Environ.* **67**, 252–277 (2013).

66. Azarmi, F. *et al.* Physicochemical characteristics and occupational exposure to coarse, fine and ultrafine particles during building refurbishment activities. *J. Nanoparticle Res. 2015 178* **17**, 1–19 (2015).

67. Kulaksiz, S. & Bau, M. Contrasting behaviour of anthropogenic gadolinium and natural rare earth elements in estuaries and the gadolinium input into the North Sea. *Earth Planet. Sci. Lett.* **260**, 361–371 (2007).

68. Lawrence, M. G. *et al.* Aquatic geochemistry of the rare earth elements and yttrium in the Pioneer River catchment, Australia. *Mar. Freshw. Res.* **57**, 725–736 (2006).

69. Brock, T., Groteklaes, M. & Mischke, P. European Coatings Handbook. *Eur. Coatings Handb.* (2019). doi:10.1515/9783748602255/HTML

70. IARC Working Group on the Evaluation of Carcinogenic Risks To Humans. *Chemical Agents and Related Occupations, IARC Monographs on the Evaluation of Carcinogenic Risks to Humans*. (IARC, 2012).

71. Chen, J., Xiao, Y., Huang, B. & Sun, X. Sustainable cool pigments based on iron and tungsten co-doped lanthanum cerium oxide with high NIR reflectance for energy saving. *Dye. Pigment.* **154**, 1–7 (2018).

72. Böhlandt, A. *et al.* High concentrations of cadmium, cerium and lanthanum in indoor air due to environmental tobacco smoke. *Sci. Total Environ.* **414**, 738–741 (2012).

73. Binnemans, K., Jones, P. T., Müller, T. & Yurramendi, L. Rare Earths and the Balance Problem: How to Deal with Changing Markets? *J. Sustain. Metall. 2018 41* **4**, 126–146 (2018).

74. American elements. Lanthanum Nanoparticles | AMERICAN ELEMENTS ® | CAS 7439-91-0. Available at: https://www.americanelements.com/lanthanum-nanoparticles-7439-91-0. (Accessed: 10th September 2021)

75. Baranowska-Wójcik, E., Szwajgier, D., Oleszczuk, P. & Winiarska-Mieczan, A. Effects of Titanium Dioxide Nanoparticles Exposure on Human Health—a Review. *Biol. Trace Elem. Res. 2019 1931* **193**, 118–129 (2019).

76. Adgate, J. L. *et al.* Relationships between personal, indoor, and outdoor exposures to trace elements in PM2.5. *Sci. Total Environ.* **386**, 21–32 (2007).

77. Kuruvilla, L. & Cheranellore Kartha, C. Cerium depresses endocardial endothelial cell-mediated proliferation of cardiac fibroblasts. *Biol. Trace Elem. Res. 2006 1141* **114**, 85–92 (2006).

78. Gómez-Aracena, J. *et al.* Toenail cerium levels and risk of a first acute myocardial infarction: The EURAMIC and heavy metals study. *Chemosphere* **64**, 112–120 (2006).

79. Kim, I. S., Baek, M. & Choi, S. J. Comparative Cytotoxicity of Al 2O 3, CeO 2, TiO 2and ZnO nanoparticles to human lung cells. *J. Nanosci. Nanotechnol.* **10**, 3453–3458 (2010).

80. Cassee, F. R. *et al.* Exposure, Health and Ecological Effects Review of Engineered Nanoscale Cerium and Cerium Oxide Associated with its Use as a Fuel Additive. *http://dx.doi.org/10.3109/10408444.2010.529105* **41**, 213–229 (2011).

81. Vocaturo, G. *et al.* Human Exposure to Heavy Metals: Rare Earth Pneumoconiosis in Occupational Workers. *Chest* **83**, 780–783 (1983).

82. Ahamed, M., Akhtar, M. J., Majeed Khan, M. A., Alaizeri, Z. M. & Alhadlaq, H. A. Evaluation of the Cytotoxicity and Oxidative Stress Response of CeO 2-RGO Nanocomposites in Human Lung Epithelial A549 Cells. (2019). doi:10.3390/nano9121709

83. Sisler, J. D. *et al.* Toxicological Assessment of CoO and La2O3 Metal Oxide Nanoparticles in Human Small Airway Epithelial Cells. *Toxicol. Sci.* **150**, 418–428 (2016).

84. Lim, C. H. Toxicity of Two Different Sized Lanthanum Oxides in Cultured Cells and Sprague-Dawley

Rats. *Toxicol. Res. 2015 312* **31**, 181–189 (2015).

85. US EPA. *Toxicological review of Cerium Oxide and Cerium Compounds. In Support of Summary Information on the Integrated Risk Information System (IRIS)*. (2009).

86. Jochum, K. P. *et al.* Reference Values Following ISO Guidelines for Frequently Requested Rock Reference Materials. *Geostand. Geoanalytical Res.* **40**, 333–350 (2016).

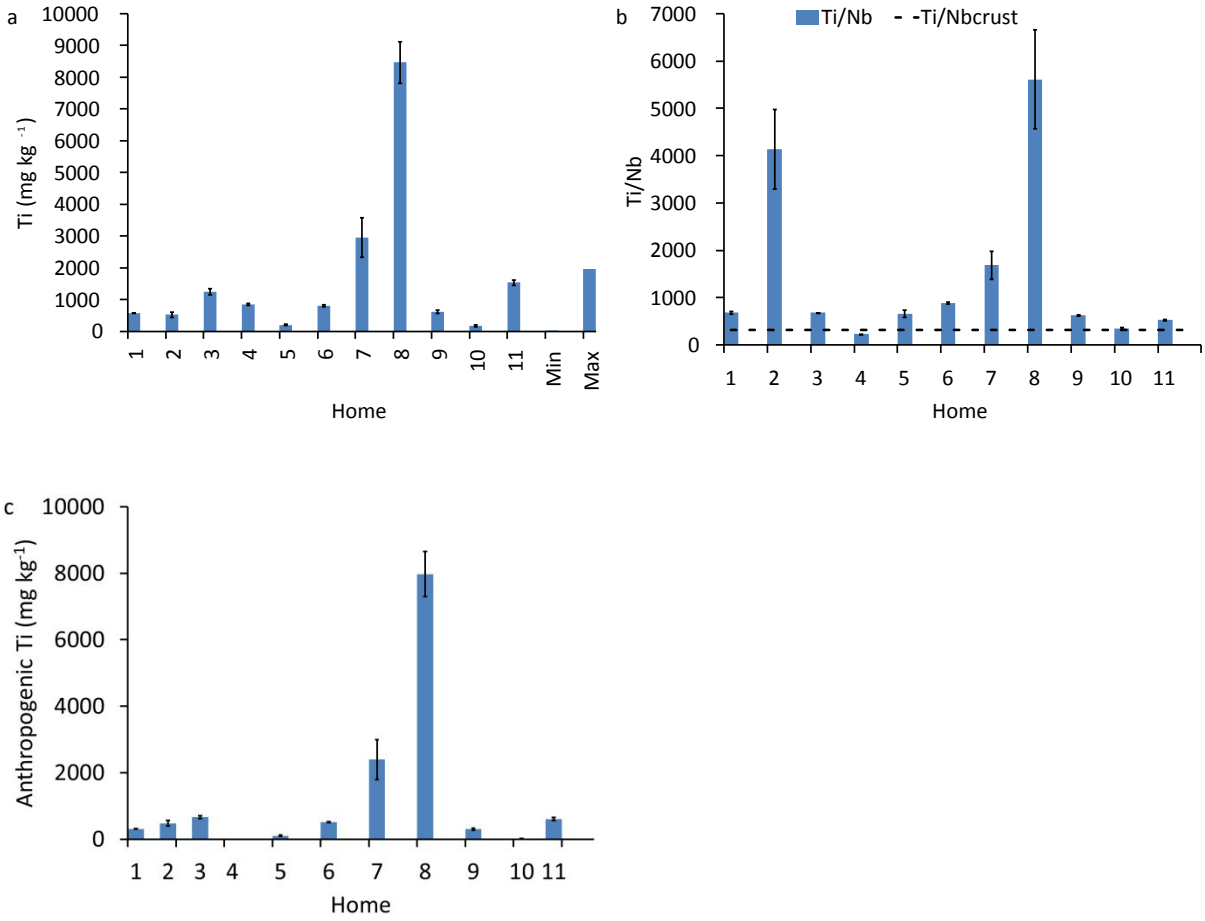

Figure 1. (a) Titanium concentrations (b) Ti/Nb, and (c) anthropogenic TiO_2 concentrations in bulk home dusts collected from the surface of heating, ventilation, and air conditioning (HVAC) units from residential homes. Min and Max refer to the minimum and maximum Ti concentrations detected in the five black HVAC filters. Concentrations are presented as mean ± standard deviation of three replicates.

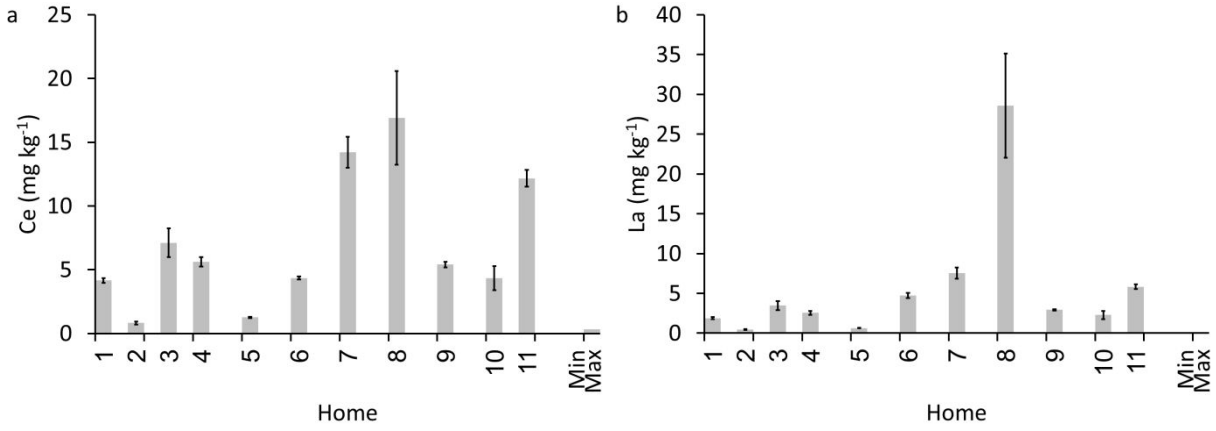

Figure 2. Concentrations of (a) Ce and (b) La in bulk home dusts collected from the surface of heating, ventilation, and air conditioning (HVAC) units from residential homes. Min and Max refer to the minimum and maximum concentrations detected in the five blank HVAC filters.

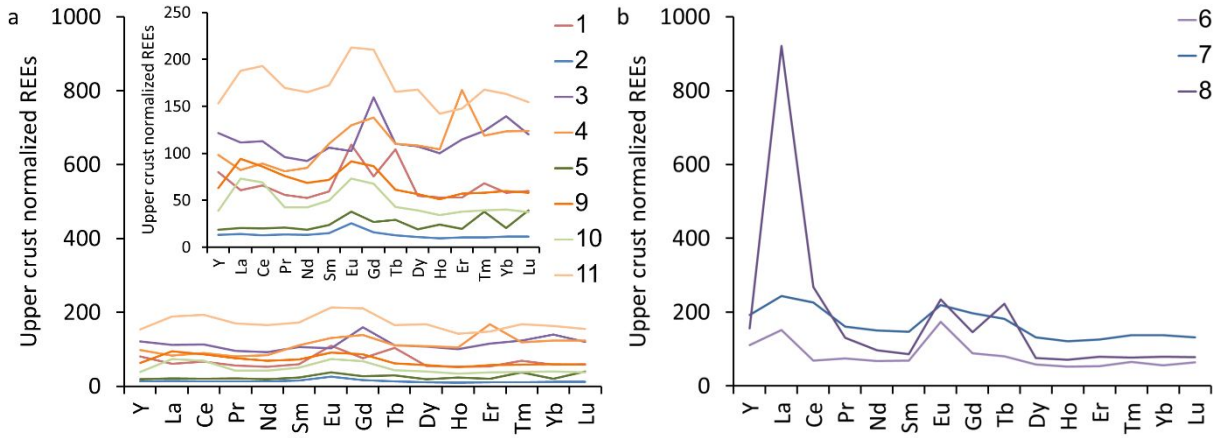

Figure 3. Upper crust normalized rare earth element concentrations in bulk home dusts collected from the surface of heating, ventilation, and air conditioning (HVAC) units from residential homes: (a) homes 1, 2, 3, 4, 5, 9, 10, and 11 display a similar pattern to upper average crust and (b) 6, 7, and 8 show enrichment in Ce, and La.

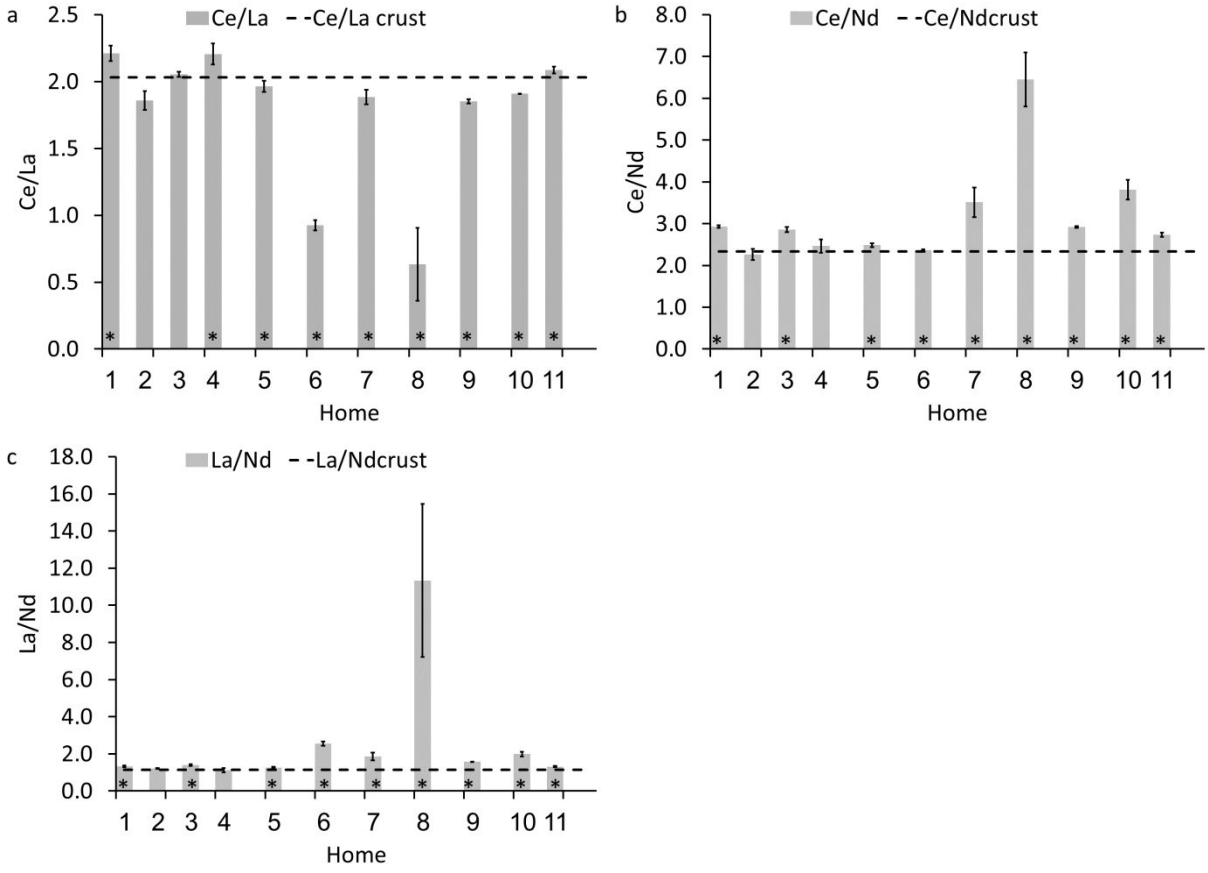

Figure 4. Elemental ratios of (a) Ce/La, (b) Ce/Nd, and (c) La/Nd in bulk home dusts collected from the surface of heating, ventilation, and air conditioning (HVAC) units from residential homes. * indicates significantly different (t-test) values relative to average crustal Ce/La, Ce/Nd, and La/Nd.

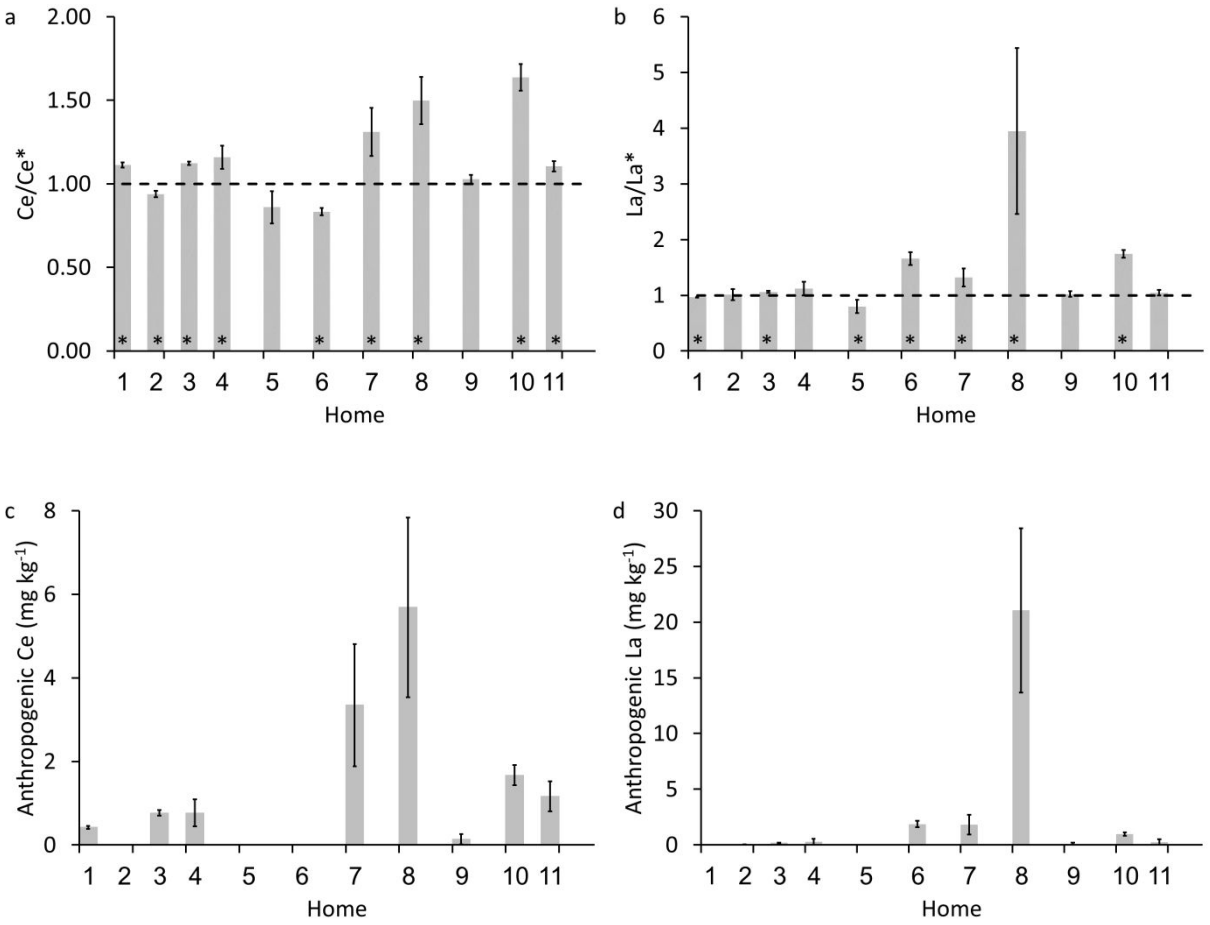

Figure 5. (a) Ce and (b) La anomalies in bulk home dusts collected from the surface of heating, ventilation, and air conditioning (HVAC) units from residential homes. Concentrations of anthropogenic (c) Ce and (d) La. * indicates significantly different (t-test) values relative to Ce/Ce* and La/La* of 1.

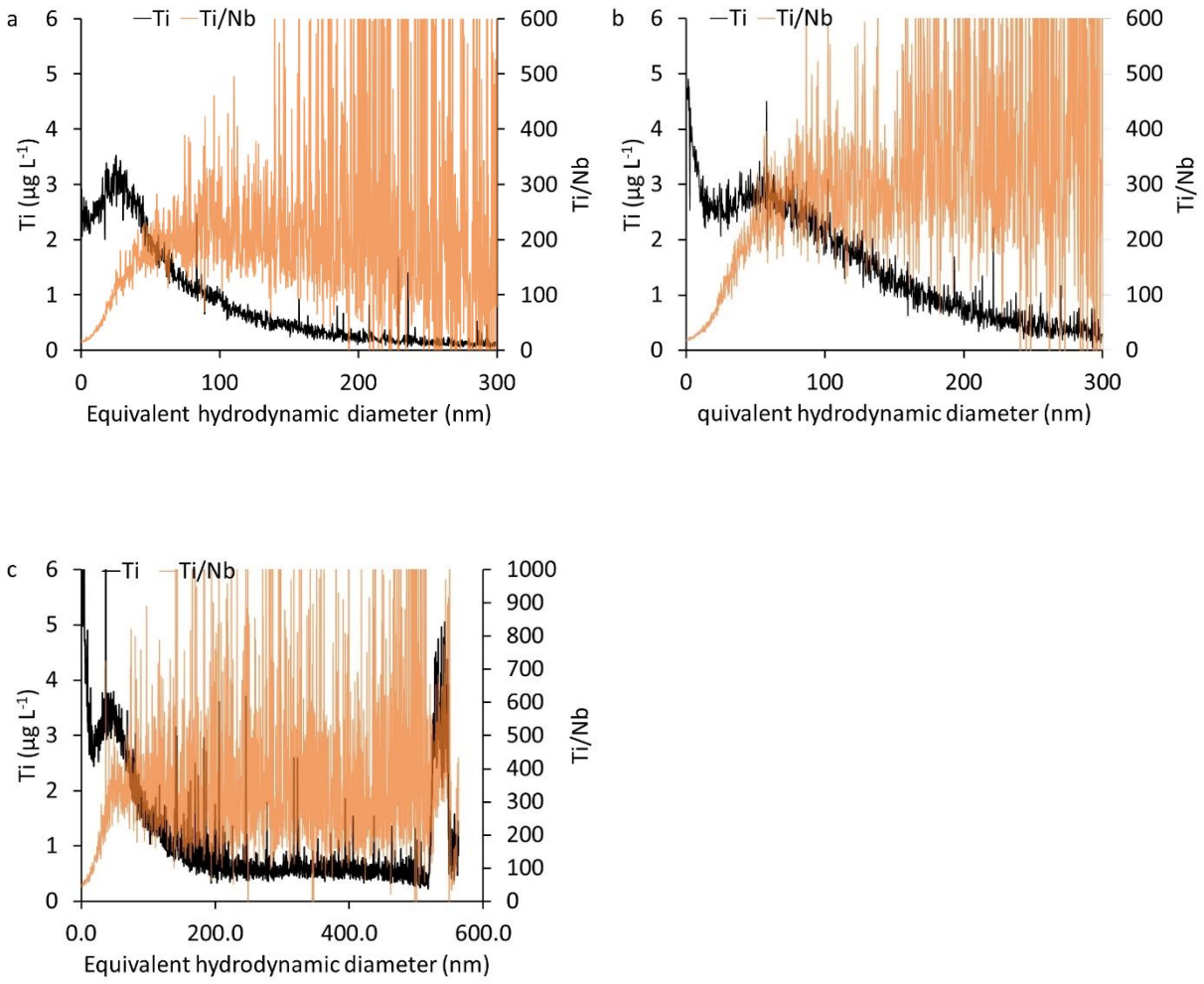

Figure 6. Size-based Ti concentration and Ti/Nb elemental ratio distributions in the < 450 nm extracted particle fractions from dusts collected from homes (a) 4, (b) 7, and (c) 8. Particles were fractionated using asymmetrical flow-field flow fractionation (AF4) and metals were analyzed by inductively coupled plasma-mass spectrometry (ICP-MS).

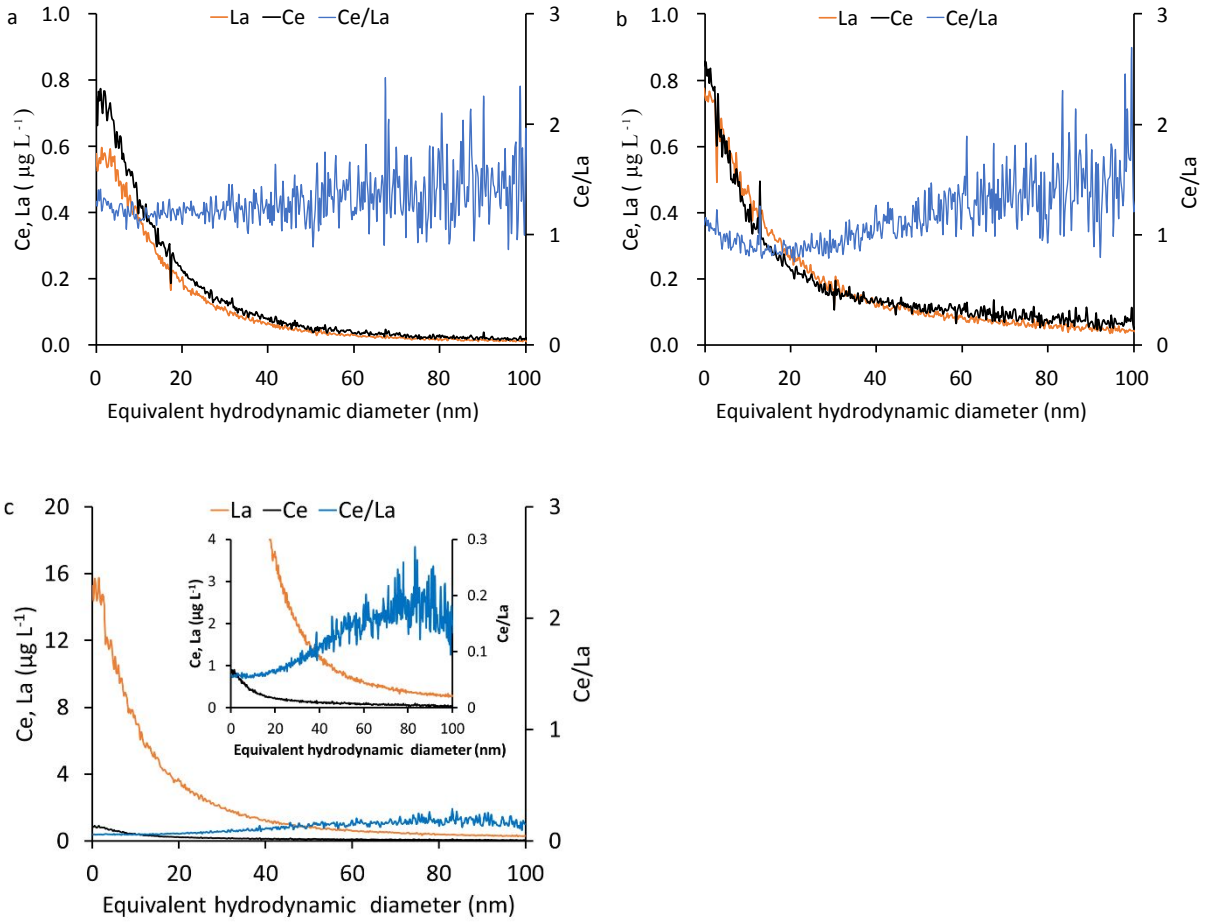

Figure 7. Size-based La concentration and Ce/La elemental ratio distributions in the < 450 nm extracted particle fractions from dusts collected from homes (a) 4, (b) 7, and (c) 8. Particles were fractionated using asymmetrical flow-field flow fractionation (AF4) and metals were analyzed by inductively coupled plasma-mass spectrometry (ICP-MS).

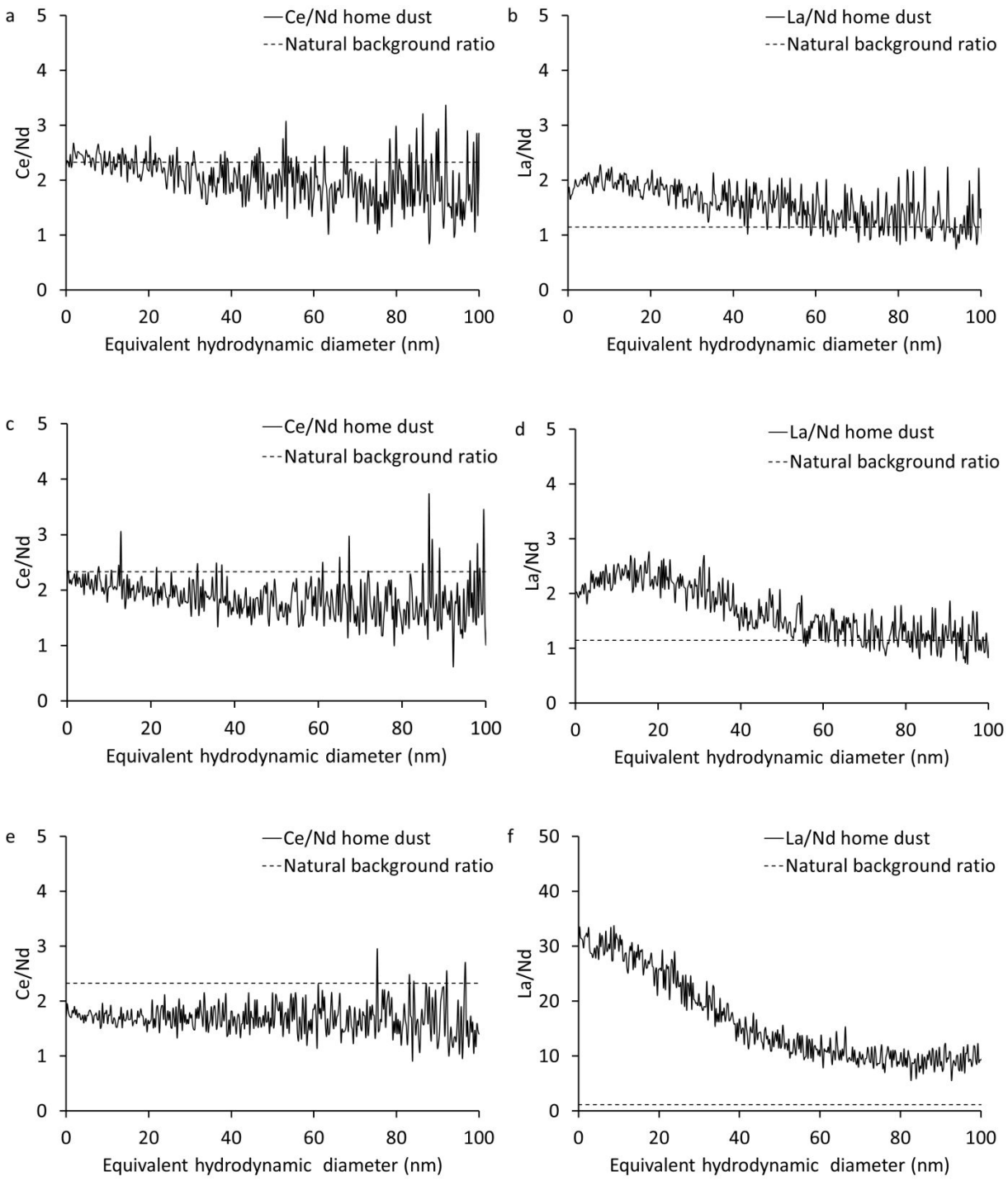

Figure 8. Size-based elemental ratios of (a, c, and e) Ce/Nd and (b, d, f) La/Nd in the extracted particles < 450 nm fractions from dusts collected from homes (a, b) 4, (c, d) 7, and (f, e) 8. Particles were fractionated using asymmetrical flow-field flow fractionation (AF4) and metals were analyzed by inductively coupled plasma-mass spectrometry (ICP-MS).